Charged Current Gauge Couplings

G. Bella[a]

[a]School of Physics and Astronomy,
Raymond and Beverly Sackler Faculty of Exact Sciences,
Tel Aviv University, 69978 Tel Aviv, Israel

The LEP measurements of charged current triple and quartic gauge couplings are described. LEP combined limits for anomalous quartic gauge couplings are presented. The combination of LEP triple gauge coupling results is pending full understanding of the recently calculated $\mathcal{O}(\alpha)$ radiative effects. The W polarization has been measured at LEP and the results agree with the standard model predictions.

1. INTRODUCTION

The Standard Model (SM), due to its non-Abelian nature, predicts self interactions between the electroweak gauge bosons, γ, W and Z. These interactions always involve the W boson and lead to the triple gauge vertices WWγ, WWZ and the quartic gauge vertices WW$\gamma\gamma$, WWZγ, WWZZ and WWWW. To test the SM, the LEP experiments measure the Triple Gauge Couplings (TGC) of the WWγ and WWZ vertices and also search for anomalous couplings not predicted by the SM which could contribute to these vertices. For Quartic Gauge Couplings (QGCs) the SM contributions are too small to be measured at LEP2 energies with the available statistics and only much larger limits on anomalous contributions can be obtained.

The most general effective Lagrangian involving the WWγ or WWZ vertices [1,2] has 14 terms with the C- and P-conserving couplings g_1^V, κ_V, λ_V; C- and P-violating couplings g_5^V; C-violating and P-conserving couplings g_4^V; C-conserving and P-violating $\tilde{\kappa}_V$ and $\tilde{\lambda}_V$. In all these couplings, $V = \gamma$,Z. According to the SM, $g_1^V{=}\kappa_V{=}1$, whereas all other couplings vanish. Therefore, $\Delta g_1^V = g_1^V - 1$ and $\Delta\kappa_V = \kappa_V - 1$ and all other couplings are considered as anomalous. From QED gauge invariance, $g_1^\gamma = 1$. Precision measurements at the Z resonance and lower energy data are consistent with the following SU(2)$\times$U(1) relations,

$$\Delta\kappa_z = -\Delta\kappa_\gamma \tan^2\theta_w + \Delta g_1^z, \qquad \lambda_z = \lambda_\gamma, \tag{1}$$

and most of the effort at LEP is the measurement of $\Delta\kappa_\gamma$, Δg_1^z and λ_γ assuming these relations. Similar relations between some of the CP violating TGC, namely, $\tilde{\kappa}_Z{=}\tilde{\kappa}_\gamma \tan^2\theta_w$, $\tilde{\lambda}_Z{=}\tilde{\lambda}_\gamma$, are also assumed in some analyses.

Some of the theoretical models leading to anomalous TGC give also anomalous contributions to quartic gauge vertices. However, it is much easier to constrain these contributions by measuring the corresponding contributions to TGC. Therefore, in the study of quartic gauge vertices we consider only genuine anomalous QGCs which are not involved with any contribution to TGC. There are two CP conserving couplings, a_0^W, a_c^W, corresponding to the WW$\gamma\gamma$ vertex [3] and one CP violating coupling, a_n^W, which corresponds to the WWZγ vertex [4]. The other quartic gauge vertices are not accessible at LEP2 energies.

2. TGC FROM W-PAIRS

W-pair production is the main process used at LEP for the study of charged current TGC due to the contribution from the diagram in Fig. 1a. W-pair events are selected by the LEP experiments with all possible final states, namely $\mathrm{q\overline{q}q\overline{q}}$, $\mathrm{q\overline{q}}\ell\overline{\nu}_\ell$ and $\ell\overline{\nu}_\ell\ell'\nu_{\ell'}$, where $\ell = \mathrm{e}, \mu, \tau$. The typical efficiency varies between 70% for $\ell\overline{\nu}_\ell\ell'\nu_{\ell'}$, $\mathrm{q\overline{q}}\tau\overline{\nu}_\tau$,

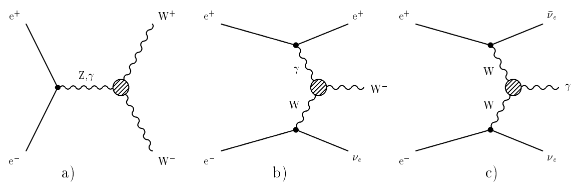

Figure 1. Feynman diagrams including the triple gauge vertex

and 90% for the other channels, with purity at the level of 80-90%. The total W-pair cross-section, the angular distribution and the polarization of the W bosons are sensitive to TGC. Consequently, there are five relevant kinematic variables, namely the W^- production angle, $\cos\theta_{\rm W}$, and the decay angles of the W^-, $\cos\theta_1^*$,ϕ_1^*, and W^+, $\cos\theta_2^*$,ϕ_2^*, in the rest-frame of the parent W. There is, however, some ambiguity in the reconstruction of these angles depending on the decay channels of the W bosons.

The total W-pair cross-section is a second-order polynomial in the TGC, so that its measurement yields directly constraints on the TGC. On the other hand, the utilization of the five kinematic variables is more complicated and the experiments are using different methods. The most direct method is a five-dimensional likelihood fit in these variables, fitting the theoretical prediction to the data. This prediction is obtained either from Monte Carlo (MC) (L3 [5]) or from the analytic Born-level expression (ALEPH [6]) correcting for initial state radiation, detector resolution, efficiency and background.

Another method to extract the TGC uses Optimal Observables (OO) based on the second-order polynomial dependence of the differential cross-section on the couplings,

$$\frac{d\sigma}{d\Omega} = S^{(0)}(\Omega) + \sum_i \alpha_i S_i^{(1)}(\Omega) + \sum_{i,j} \alpha_i \alpha_j S_{ij}^{(2)}(\Omega).$$

Here Ω is the 5D phase-space point, Ω=($\cos\theta_{\rm W}$,$\cos\theta_1^*$,ϕ_1^*,$\cos\theta_2^*$,ϕ_2^*) and α_i are the anomalous TGC. The OO, defined as $\mathcal{O}_i^{(1)}$=$S_i^{(1)}(\Omega)/S^{(0)}(\Omega)$, $\mathcal{O}_{ij}^{(2)}$=$S_{ij}^{(2)}(\Omega)/S^{(0)}(\Omega)$ contain all the relevant information needed to extract the couplings [7]. As an example, Fig. 2 shows the $\mathcal{O}^{(1)}_{\Delta g_1^{\rm z}}$ distribution for $\rm q\bar{q}q\bar{q}$ events at 189 GeV measured by DELPHI.

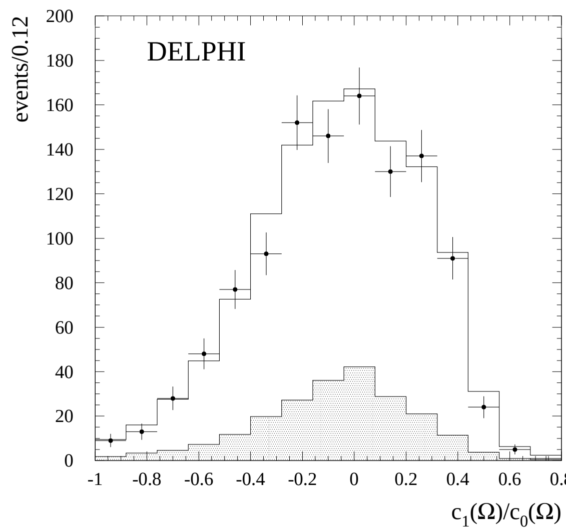

Figure 2. DELPHI $\mathcal{O}^{(1)}_{\Delta g_1^{\rm z}}$ distribution

In a fit where only one coupling, α_i, is extracted, assuming all other anomalous TGC to vanish, only two optimal observables, $\mathcal{O}_i$, $\mathcal{O}_{ii}$ are needed. However, when n couplings are fitted simultaneously, the number of relevant observables increases according to n+n(n+1)/2 and for $n > 2$ the whole method becomes impractical. For n=2 (5 OO) a multi-dimensional clustering technique is used by DELPHI [8] for the fit. Another approach is based on the assumption that the anomalous couplings are small, in which case, they can be extracted just from the mean values of the OOs rather than the full OO distributions, as done by ALEPH [9] and OPAL [10].

A third method to extract the TGC is based on the measurement of the Spin Density Matrix (SDM) elements which will be discussed in the next section.

On summer 2000 a combination of the LEP results have been performed [11] using data at centre-of-mass energies up to 202 GeV and taking into account correlations between systematic errors of the four LEP experiments due to the uncertainty in the theoretical total cross-section value (2%) and in the fragmentation models. The errors obtained for $\Delta\kappa_\gamma$, Δg_1^z and λ_γ were 0.066, 0.026 and 0.028 respectively. Since then, new MC programs [12] which include an almost complete treatment of $\mathcal{O}(\alpha)$ radiative effects and an improved Coulomb correction have become available. These programs predict a total W-pair cross-section lower by 2.5% than the old predictions, in agreement with the LEP measurements, with an improved precision of 0.5%. On the other hand, the $\cos\theta_{\mathrm{w}}$ distribution in the new MC programs is steeper by 1–2% compared with the old ones, yielding a significant effect on the TGC results. This effect is still under investigation by the LEP collaborations.

Table 1
ALEPH TGC results

Coupling	TGC result	95% C.L.
$\Delta\kappa_\gamma$	$-0.020^{+.078}_{-.072}$	$[-0.164,\ 0.132]$
Δg_1^z	$0.015^{+.035}_{-.032}$	$[-0.048,\ 0.080]$
λ_γ	$-0.001^{+.034}_{-.031}$	$[-0.059,\ 0.065]$

Preliminary results based on the new MC programs were available this summer by ALEPH only [6] and no new combination have been performed since summer 2000. The ALEPH results for $\Delta\kappa_\gamma$, Δg_1^z and λ_γ, using their full LEP2 data sample and including also information from the single W and single photon final states (see below), are listed in Table 1. The corresponding log-likelihood plots are shown in Fig. 3. Aleph obtains also results for the 10 C- or P-violating couplings without using the SU(2)×U(1) constraints. All results are consistent with zero according to the SM predictions.

3. W-POLARIZATION

Measurement of the W-polarization is a model-independent way to test the SM. L3 [13] uses the $\cos\theta_\ell^*$ distribution in $q\overline{q}\ell\overline{\nu}_\ell$ events to measure the fraction of W-bosons produced at each helicity state. The results are consistent with the SM expectations as listed in Table 2. L3 also obtains evidence for spin correlations between the two W-bosons. Looking separately at samples where the hadronically decaying W is enriched (requiring $0.66 < |\cos\theta_q^*| < 1$) or depleted ($0 < |\cos\theta_q^*| < 0.33$) in transversely-polarized W a difference at a level of 3.6σ is found between the $\cos\theta_\ell^*$ distributions of the two samples, as shown in Fig. 4

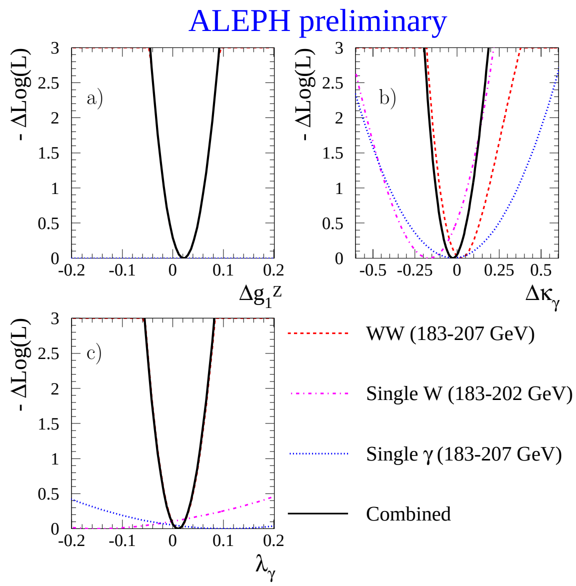

Figure 3. Preliminary log-likelihood plots for $\Delta\kappa_\gamma$, Δg_1^z and λ_γ obtained by ALEPH

Table 2
Preliminary L3 W-polarization results at $\sqrt{s}$=206.6 GeV and SM predictions

	Data	SM
σ_-/σ_{tot}	$0.647 \pm .066$	0.623
σ_+/σ_{tot}	$0.137 \pm .034$	0.157
σ_L/σ_{tot}	$0.216 \pm .053$	0.220

OPAL [14] and DELPHI [15] measure the ele-

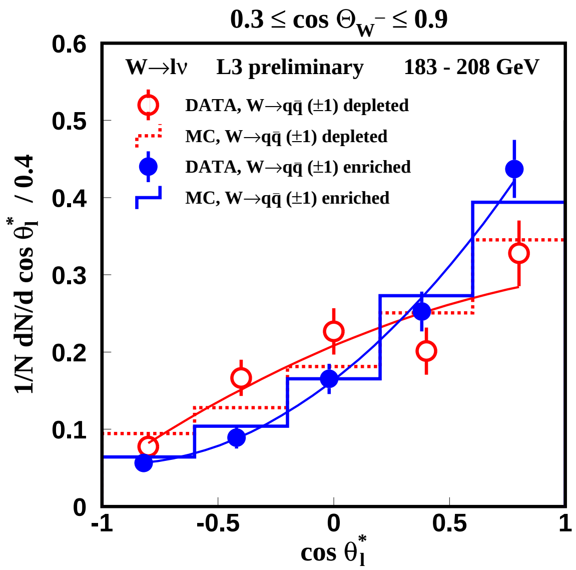

Figure 4. L3 evidence for WW spin correlations (see text)

ments of the SDM defined by,

$$\rho_{\tau_-\tau'_-\tau_+\tau'_+}(s,\cos\theta_{\mathrm{W}}) = \frac{\sum_\lambda F^{(\lambda)}_{\tau_-\tau_+}(F^{(\lambda)}_{\tau'_-\tau'_+})^*}{\sum_{\lambda\tau_+\tau_-}|F^{(\lambda)}_{\tau_-\tau_+}|^2}$$

where $F^{(\lambda)}_{\tau_-\tau_+}$ are the helicity amplitudes to produce $\mathrm{W}^-\mathrm{W}^+$ with helicities τ_-, τ_+ respectively, and λ is the helicity of the incoming electron beam. This is a 9×9 complex Hermitian matrix with trace=1, but usually one considers the one-sided SDM, $\rho^{W^-}_{\tau_-\tau'_-} = \sum_{\tau_+}\rho_{\tau_-\tau'_-\tau_+\tau_+}$ which is a 3×3 matrix with the same properties. CPT invariance at the tree level corresponds to the relation $\rho^{W^-}_{\tau_1\tau_2} = (\rho^{W^+}_{-\tau_1-\tau_2})^*$ and CP invariance yields $\rho^{W^-}_{\tau_1\tau_2} = \rho^{W^+}_{-\tau_1-\tau_2}$. This allows to check in a model-independent way for CPT or CP violation in W-pair production. Fig. 5 shows the various SDM elements vs. $\cos\theta_{\mathrm{W}}$ as measured by OPAL using the leptonically decaying W in $\mathrm{q\overline{q}}\ell\overline{\nu}_\ell$ event at 189 GeV. These are used to constrain the CP-violating TGC, which are found to be consistent with zero, as expected by the SM. Averaging the diagonal SDM elements over $\cos\theta_{\mathrm{W}}$, using both W bosons from $\mathrm{q\overline{q}}\ell\overline{\nu}_\ell$ events, OPAL obtains the W-polarization results listed in Table 3. Using also the two-side SDM elements, OPAL obtains the probabilities for the two-W polarization states TT, LL and TL (Table 3).

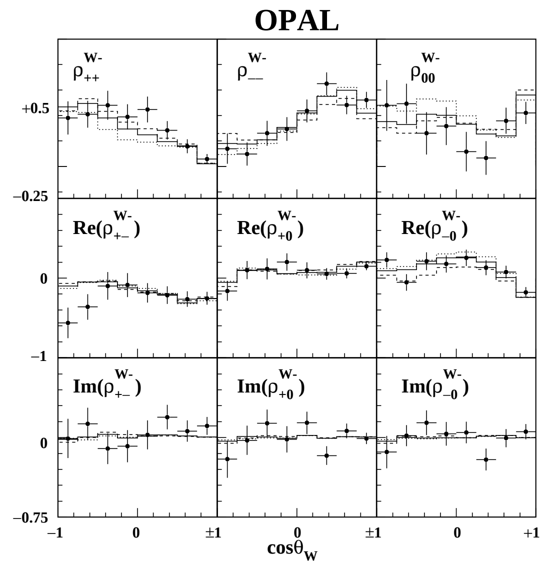

Figure 5. SDM elements measured by OPAL

Table 3
OPAL W-polarization results at $\sqrt{s}$=189 GeV and SM predictions

	Data	SM
σ_T/σ_{tot}	$0.790 \pm .033 \pm .016$	0.743
σ_L/σ_{tot}	$0.210 \pm .033 \pm .016$	0.257
σ_{TT}/σ_{tot}	$0.781 \pm .090 \pm .033$	0.572
σ_{LL}/σ_{tot}	$0.201 \pm .072 \pm .018$	0.086
σ_{TL}/σ_{tot}	$0.018 \pm .147 \pm .038$	0.342

4. TGC FROM SINGLE W AND SINGLE PHOTON

The processes $\mathrm{e^+e^-}\to\mathrm{We}\nu$ and $\mathrm{e^+e^-}\to\nu\overline{\nu}\gamma$ have some sensitivity to TGC due to the contributions from the diagrams in Figs. 1b and 1c respectively. In both processes, the sensitivity is only to the WWγ couplings, whereas in W-pair production there is also a contribution from the WWZ vertex, and both contributions cannot be separated. However, in the case of $e^+e^-\to We\nu$ there is high ($\approx$50%) background which is mainly from W-pair events, resulting in some sensitivity of the event sample to the WWZ vertex. In this process, the final state electron escapes undetected into the beam-pipe and only the single W leaves a signature in the detector. In the case of hadronic W-decays, two jets are visible, whereas for leptonic decays only a single lepton is observed. In both cases, there is large missing energy and momentum. The main sensitivity to TGC comes from the total event rate, but also some information from differential distributions is used. All experiments assume the SU(2)$\times$U(1) relations (1) between the WWγ and WWZ couplings, and the results [8,16] are listed in Table 4. These results are less precise than those from W-pair events, but they still have some non-negligible effect in constraining the upper limit for $\Delta\kappa_\gamma$.

Table 4
LEP results (95% C.L. limits for ALEPH) on TGC from single W events

Exp.	Data	$\Delta\kappa_\gamma$	λ_γ
ALEPH	161–202	[−0.54, 0.15]	[−0.57, 0.44]
DELPHI	189,lept.	$0.23^{+0.33}_{-0.39}$	$0.48^{+0.39}_{-1.29}$
DELPHI	189,hadr.	$0.19^{+0.36}_{-0.58}$	$0.42^{+0.39}_{-1.21}$
L3	161-202	0.10 ± 0.13	$-0.20^{+0.60}_{-0.19}$
OPAL	189	$0.06^{+0.17}_{-0.19}$	$-0.44^{+0.43}_{-0.24}$

The process $e^+e^-\to\nu\bar{\nu}\gamma$ is even less sensitive to TGC than the single W production. The main sensitivity is for energetic photons with large angle to the beam-pipe. Therefore, in addition to the total rate, the experiments use also the energy spectrum and the angular distribution of the photon to constrain the TGC. Here the sensitivity is only to $\Delta\kappa_\gamma$ and λ_γ without any contribution from the WWZ vertex. The results [5,6,8,17] are listed in Table 5.

Table 5
LEP results (95% C.L. limits for L3) on TGC from single photon events

Exp.	Data	$\Delta\kappa_\gamma$	λ_γ
ALEPH	183–208	$-0.05^{+0.30}_{-0.25}$	$0.10^{+0.35}_{-0.35}$
DELPHI	189	$0.70^{+0.77}_{-0.99}$	$0.65^{+1.03}_{-1.79}$
L3	189-202	[−2.7, 0.8]	[−1.6, 1.7]
OPAL	189-202	$-0.15^{+1.07}_{-1.03}$	$-0.18^{+1.38}_{-1.34}$

The experiments combine their results from the single W and single photon productions with those from W-pair production by summing the corresponding log-likelihood functions. The Aleph results on $\Delta\kappa_\gamma$ and λ_γ in Table 1 include already the information from these two processes.

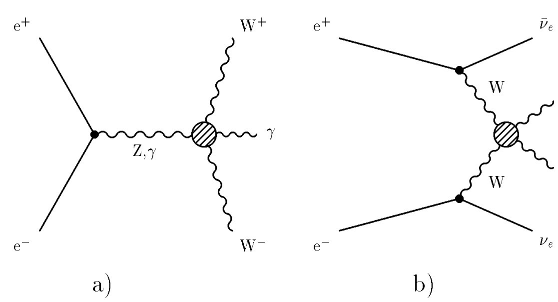

Figure 6. Feynman diagrams including the quartic gauge vertex

5. QUARTIC GAUGE COUPLINGS

The Feynman diagrams in Fig. 6 contain the quartic gauge vertex. The process $e^+e^-\to WW\gamma$ is sensitive to all three couplings, a_0^W, a_c^W and a_n^W. Most of the sensitivity is for energetic photon which is away from the beam-pipe direction, in contrast to initial state radiation which gives the dominant contribution to the WWγ final state, where the photon tends to be along the incoming beams with low energy. Therefore, in addition to the total yield of WWγ events, the photon spectrum is also used and OPAL uses the photon angular distribution as well.

Table 6
LEP 95% C.L. limits on QGC

	a_0^W/Λ^2	a_c^W/Λ^2	a_n^W/Λ^2
ALEPH	[−0.029, 0.029]	[−0.079, 0.080]	
L3	[−0.017, 0.017]	[−0.03, 0.05]	[−0.15, 0.14]
OPAL	[−0.065, 0.065]	[−0.13, 0.17]	[−0.61, 0.57]
LEP	[−0.018, 0.018]	[−0.033, 0.047]	[−0.17, 0.15]

The process $e^+e^- \to \nu\overline{\nu}\gamma\gamma$ involves only the WW$\gamma\gamma$ vertex and is then sensitive only to a_0^W and a_c^W. This sensitivity is lower than the previous process. A cut is imposed on $M_{\nu\overline{\nu}}$ to be below the Z^0 region in order to reject Z$\gamma\gamma$ events. Results from both channels and from three LEP experiments, ALEPH, L3 and OPAL, are combined by adding the corresponding log-likelihood functions. Fig. 7 shows the resulting log-likelihood curves and Table 6 lists the corresponding 95% C.L. limits [18]. All the results are consistent with the absence of anomalous QGC.

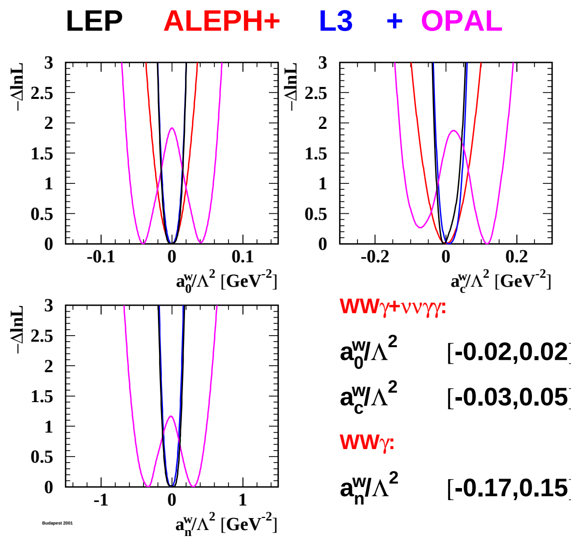

Figure 7. QGC log-likelihood curves

REFERENCES

1. K. Hagiwara *et al*, *Nucl. Phys.* B **282** (1987) 253.
2. Physics at LEP2, edited by G. Altarelli *et al*, CERN 96-01 Vol. 1, 525.
3. G. Bélanger and F. Boudjema, *Phys. Lett.* B **288** (1992) 201.
4. O.J.P. Eboli *et al*, *Nucl. Phys.* B **411** (1994) 381.
5. L3 Collaboration, L3 Note 2567.
6. ALEPH Collaboration, ALEPH 2001-060, CONF 2001-040.
7. G.K. Fanourakis, D. Fassouliotis and S.E. Tzamarias, *Nucl. Instrum. Methods* A **412** (1998) 465; *Nucl. Instrum. Methods* A **414** (1998) 399.
8. DELPHI Collaboration, *Phys. Lett.* B **502** (2001) 9.
9. ALEPH Collaboration, *Eur. Phys. J.* C **21** (2001) 423.
10. OPAL Collaboration, *Eur. Phys. J.* C **19** (2001) 1; OPAL Physics Note PN441.
11. The LEP Collaborations ALEPH, DELPHI, L3, OPAL, and the LEP TGC Working group, LEPEWWG/TGC/2000-02
12. A. Denner *et al*, *Phys. Lett.* B **475** (2000) 127; S. Jadach *et al*, *Phys. Rev.* D **61** (2000) 113010.
13. L3 Collaboration, L3 Note 2636.
14. OPAL Collaboration, *Eur. Phys. J.* C **19** (2001) 229.
15. DELPHI Collaboration, DELPHI 2001-098 CONF 526.
16. ALEPH Collaborations, ALEPH 2000-054 CONF 2000-036; L3 Collaboration, L3 Note 2518; OPAL Collaboration, OPAL Physics Note PN427.
17. OPAL Collaboration, OPAL Physics Note PN481.
18. The LEP Collaborations ALEPH, DELPHI, L3, OPAL, and the LEP GC Working group, LEPEWWG/TGC/2001-03.